Jundishapur J Nat Pharm Prod. 2018 November; 13(4):e12873. doi: 10.5812/jjnpp.12873.

Published online 2018 December 2. **Research Article**

An Alternative Approach for Improved Entrapment Efficiency of Hydrophilic Drug Substance in PLGA Nanoparticles by Interfacial Polymer Deposition Following Solvent Displacement

Sara Salatin [1, 2], Jaleh Barar [1, 3], Mohammad Barzegar-Jalali [3], Khosro Adibkia [3, 4], Farhad Kiafar [3, 5] and Mitra Jelvehgari [3, 4, *]

[1] Research Center for Pharmaceutical Nanotechnology, Tabriz University of Medical Sciences, Tabriz, Iran
[2] Student Research Committee, Tabriz University of Medical Sciences, Tabriz, Iran
[3] Department of Pharmaceutics, Faculty of Pharmacy, Tabriz University of Medical Sciences, Tabriz, Iran
[4] Drug Applied Research Center and Faculty of Pharmacy, Tabriz University of Medical Sciences, Tabriz, Iran
[5] Zahravi Pharmaceutical Company, Tabriz, Iran

[*] *Corresponding author*: Department of Pharmaceutics, Faculty of Pharmacy, Tabriz University of Medical Sciences, Tabriz, Iran. Tel: +98-4133392585, Fax: +98-4133344798, Email: jelvehgri@tbzmed.ac.ir

Received 2016 August 26; **Revised** 2017 December 12; **Accepted** 2018 January 07.

Abstract

Background: Alzheimer's disease (AD) is an age-related and irreversible neurological disorder. The low efficacy of current therapeutic strategies is related to both poor drug potency and the presence of various obstacles in the delivery routes, such as blood-brain barrier (BBB) that limits the uptake of most drugs by the brain. Rivastigmine hydrogen tartrate (RHT) is used in mild to moderate forms of AD therapy.
Objectives: The present study described the use of Poly-lactic-co-glycolic acid (PLGA) nanoparticles (NPs), as effective delivery vehicles, to improve the therapeutic efficiency of RHT.
Methods: RHT-loaded PLGA NPs were prepared using interfacial polymer deposition, following solvent displacement method with different ratios of polymer: Drug. The NPs were studied for entrapment efficiency, particle size, and surface morphology, using scanning electron microscopy (SEM), X-ray diffraction (XRD), Fourier transform infrared spectroscopy (FTIR), and differential scanning calorimetry (DSC). *In vitro* drug release from NPs was also assessed by a modified dissolution method.
Results: The entrapment efficiency of RHT in NPs was found to be between 27.71 $\pm$ 6.86 and 45.70 $\pm$ 11.06 and the average size was about 75.14 to 173 nm. The zeta potential was negative (-2.28 to -10.5 mV), as determined by dynamic light scattering (DLS). The drug released from NP formulations was between 69.98% and 89% upon 24 hours, which indicated improved sustained drug release characteristics.
Conclusions: These results suggested the potential usefulness of PLGA NPs for the delivery of RHT in a sustained and controlled manner.

Keywords: Interfacial Polymer Deposition, Nanoparticles, Rivastigmine, BBB

1. Background

Alzheimer's disease (AD) is the most popular form of age-linked degeneration of the nervous system (1). Targeting drugs into the central nervous system (CNS), to provide accurate detection and remedy of frequently occurring neurodegenerative diseases, such as AD is limited, mostly because of the presence of blood-brain barrier (BBB), which plays a significant role in protecting the CNS from free entrance of unwanted substances (2).

Polymeric nanoparticles (NPs) have certain distinct advantages, such as protection of drug from degradation and control of the rate of drug release (3, 4). It has been reported that the polymer properties, along with size and surface properties of the NPs, can affect the mechanism of their uptake by the brain capillary endothelial cells and ability to cross the epithelial cells of the BBB (5).

Poly-lactic-co-glycolic acid (PLGA) is one of the most extensive polymeric candidates applied to formulate nanoscale delivery systems, because of its biodegradability, biological adaptability, the facility of approaching a sustained drug release, and the possibility of precise modulation of their surface properties (6).

The nanoprecipitation method proposed by Fessi et al. (7) had a simple manner and has been extensively applied by different research teams to supply polymeric NPs.

Nanoprecipitation or the solvent displacement method is found on the sediment of a preformed polymer from an organic solution and the extraction of the organic solvent in the aqueous vehicle when a surfactant is present or absent (8).

Poloxamers, especially poloxamer 407®, have recently attracted great attention from various biomedical applications, such as NP stabilizers. In this work, rivastigmine hydrogen tartrate (RHT) was incorporated in the PLGA nanosuspension, using the nanoprecipitation method, with the aim of improving the loading efficiency.

2. Objectives

The aim of this article was to report on the preparation, characterization, and *in vitro* release evaluation of a biodegradable nano-particulate system of RHT, prepared through a nanoprecipitation technique employing PLGA.

3. Methods

Poly-lactic-co-glycolic acid (Resomer ® RG 503 H) and Poloxamer 407 were purchased from Sigma-Aldrich (USA). Rivastigmine hydrogen tartrate was obtained from Tofighdaru (Tehran, Iran). The dialysis bag (cut off 10000 to 12000 Da) was supplied by Biogen (Mashhad, Iran).

3.1. Nanoparticles Preparation

All formulations of the RHT and blank NPs were obtained via the nanoprecipitation method, using different polymer to drug ratios (9). To this end, 10 mg of RHT was dissolved in 2 mL of water. Different amounts of PLGA (50, 70, and 90 mg) were solved in 5 mL of acetone, separately. The RHT aqueous solution was poured dropwise in the PLGA organic solution with stirring speed of 400 rpm (Heidolph-Germany). This aqueous solution (S/W) was added to 10 mL of 2% (w/v) aqueous poloxamer 407 solution, as a suspension stabilizer. Finally, the mixture was stirred to evaporate the organic solvent.

The NPs were centrifuged (Eppendorf, Germany) at 12000 rpm for 60 minutes at 4°C (Table 1), lyophilized and stored.

3.2. Characterization of Rivastigmine Hydrogen Tartrate Nano-Particles

3.2.1. Encapsulation Efficiency and Recovery

Briefly, 5 mg of each batch of RHT NPs was separately dissolved in 10 mL of ethyl acetate. The RHT content in the precipitate of centrifuged nano-suspension was determined spectrophotometrically (UV160 Shimadzu, Japan) at 263.4 nm. The entrapment efficiency (EE), loading capacity (LC), and recovery of NPs were calculated using the following equations:

$$EE\,(\%) = \frac{Actual\ drug\ content\ in\ NPs}{Total\ drug\ used\ in\ formulation} \times 100$$

$$LC\,(\%) = \frac{Entrapped\ drug}{NPs\ weight} \times 100$$

$$NP\ recovery\,(\%) = \frac{Mass\ of\ NPs\ recovered \times 100}{Mass\ of\ all\ of\ excipients\ applied\ in\ the\ formulation}$$

3.2.2. Particle Size and Zeta Potential

The prepared nano-suspensions were characterized for the mean particle size, poly dispersity index (PDI), and zeta potential, using DLS (Malvern, UK).

3.2.3. Morphological Studies

Samples were assembled on to metal stubs and were covered with platinum/palladium alloy under vacuum, using a double-sided carbon adhesive tape. Then, a scanning electron microscope, SEM (MIRA3 TESCAN, Czech Republic), utilized at 15 kV, was applied for the morphological examination.

3.2.4. Fourier Transform Infrared Spectroscopy Analysis

Samples were examined, using a computerized FTIR (Bruker, Tensor 27, and USA) in the IR range of 400 to 4000 cm^{-1} at 1 cm^{-1} resolution.

3.2.5. Differential Scanning Calorimetry Analysis

Thermograms of samples were noted by a DSC (Shimadzu, Japan). Two milligrams of samples were placed in aluminum pans and thermograms were recorded from 25°C to 300°C, at a heating rate of 10°C/minute.

3.2.6. X-Ray Diffraction Analysis

Samples were exposed to nickel-filtered CuKα radiation (a voltage of 40 KV and a current of 20 mA) in a Bruker Axs, D8 Advance diffractometer. Scanning was performed at a rate of 2°C/minute over a 2θ range of 10°C to 90°C and with an interval of 0.02°C.

Table 1. RHT NPs Prepared by the Nano-Percipitation Method

Formulation Code	Polymer: Drug Ratio	Suspension of NPs in Aqueous Carrier (S/W)				
		Initial Aqueous Phase (S/W_1)		Organic Phase (O)		Secondary Aqueous Phase (W_2)
		Water, mL	RHT, mg	PLGA, mg	Acetone, mL q	Poloxamer (2%w/v), mL
P1	5:1	2	10	50	5	10
P2	7:1	2	10	70	5	10
P3	9:1	2	10	90	5	10
Blank P3	-	2	-	90	5	10

Abbreviaitons: RHT, Rivastigmine hydrogen tartrate; PLGA, Poly (lactic-co-glycolic acid).

3.2.7. In Vitro Release Study

Dialysis bag diffusion method was applied to investigate the RHT release *in vitro* (10). Known amounts of RHT NPs were placed in the dialysis bags, which were submersed in 200 mL of the dissolution medium (phosphate buffer, pH 7.4) in USP dissolution apparatus, with a speed of 100 rpm at 37 ± 1°C. At regular time intervals, aliquots of 3 mL were removed and displaced with a similar volume of fresh release ambiance. Then, release of drug was detected spectrophotometrically.

3.2.8. Release Kinetics

Different kinetic models, such as zero order, first order, Higuchi, Hixson Crowell, and Korsmeyer-Peppas were used to evaluate the release data obtained from the *in vitro* dissolution study.

3.2.9. Statistical Analysis

Where appropriate, release results were evaluated using One-way Analysis of Variance (ANOVA) at 0.05 level of significance.

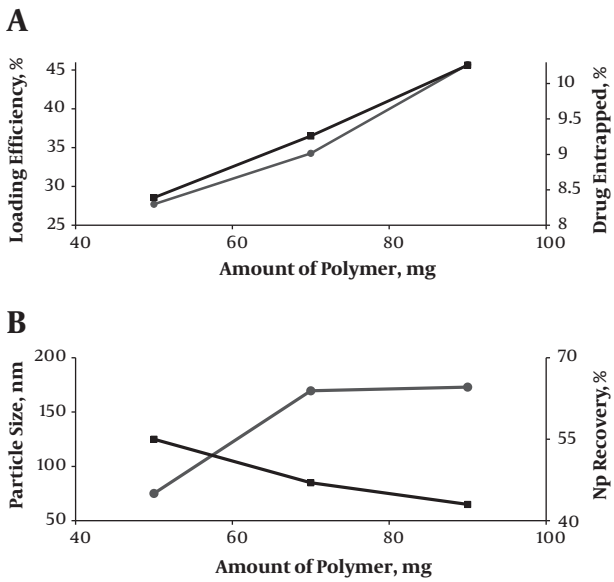

Figure 1. A) Effect of the amount of PLGA polymer on the encapsulation efficiency (●) and the loading capacity (■), B) effect of amount of PLGA polymer on mean particle size (●) and NP recovery (■).

4. Results

4.1. Preparation of Rivastigmine Hydrogen Tartrate Nano-Particles

Different RHT formulations were prepared based on the nanoprecipitation method.

4.2. Characterization of NPs

4.2.1. Loading Capacity and Entrapment Efficiency

The loading capacity and entrapment efficiency of the prepared NPs were found within the range of 8.39% to 10.62% and 27.71% to 45.70%, respectively (Table 2 and Figure 1). Therefore, the NPs with differing loading capacity, NP recovery, and particle size could be made by alteration of the amount of polymer.

4.2.2. Particle Size and Zeta Potential

The particle size of blank and RHT NPs, prepared using different polymer to drug ratios, ranged between 154 and 75.14 - 173 nm, respectively ($P > 0.05$). The zeta potential values of blank and NPs were negative (-11.1 and -2.28 to -10.5 ζ, respectively) ($P > 0.05$). Therefore, increasing average particle size and zeta potential were observed with an increment in the PLGA concentration. The mean PDI values for the blank and RHT formulations varied in the range of 0.13 and 0.095 - 0.557, respectively ($P < 0.05$) (Table 2).

4.2.3. Morphology

The results extracted from the SEM analysis indicated that the particles were predominately spherical in shape and uniform at the nanoscale scope (Figure 2).

Table 2. Effect of Drug: Polymer Ratio on Drug Loading Efficiency, Production Yield, Particle Size, Zeta Potential, and PDI of RHT NPs

Formulation Code	NP Recovery (% ± SD)	Theoretical Drug Content (%)	Mean Drug Entrapped (% ± SD)	Drug Loading Efficiency (% ± SD)	Mean Particle Size (nm)	Zeta Potential (mV ± SD)	Polydispersity Index (± SD)
P1	55	16.67	8.39 ± 2.1	27.71 ± 6.86	75.14 ± 4.28	-10.5 ± 3.02	0.095 ± 4.05
P2	47	12.5	9.26 ± 1.6	34.27 ± 1.325	169.6 ± 3.77	-7.76 ± 1.6	0.557 ± 2.49
P3	43	10	10.62 ± 3.48	45.70 ± 1.06	173 ± 5.025	-2.28 ± 2.07	0.441 ± 2.77
***blank NPs of P3**	58	-	-	-	154.7 ± 7.305	-11.1 ± 3.80	0.130 ± 1.84
RHT untreated powder	-	-	-	-	2884.03	-1.50	-

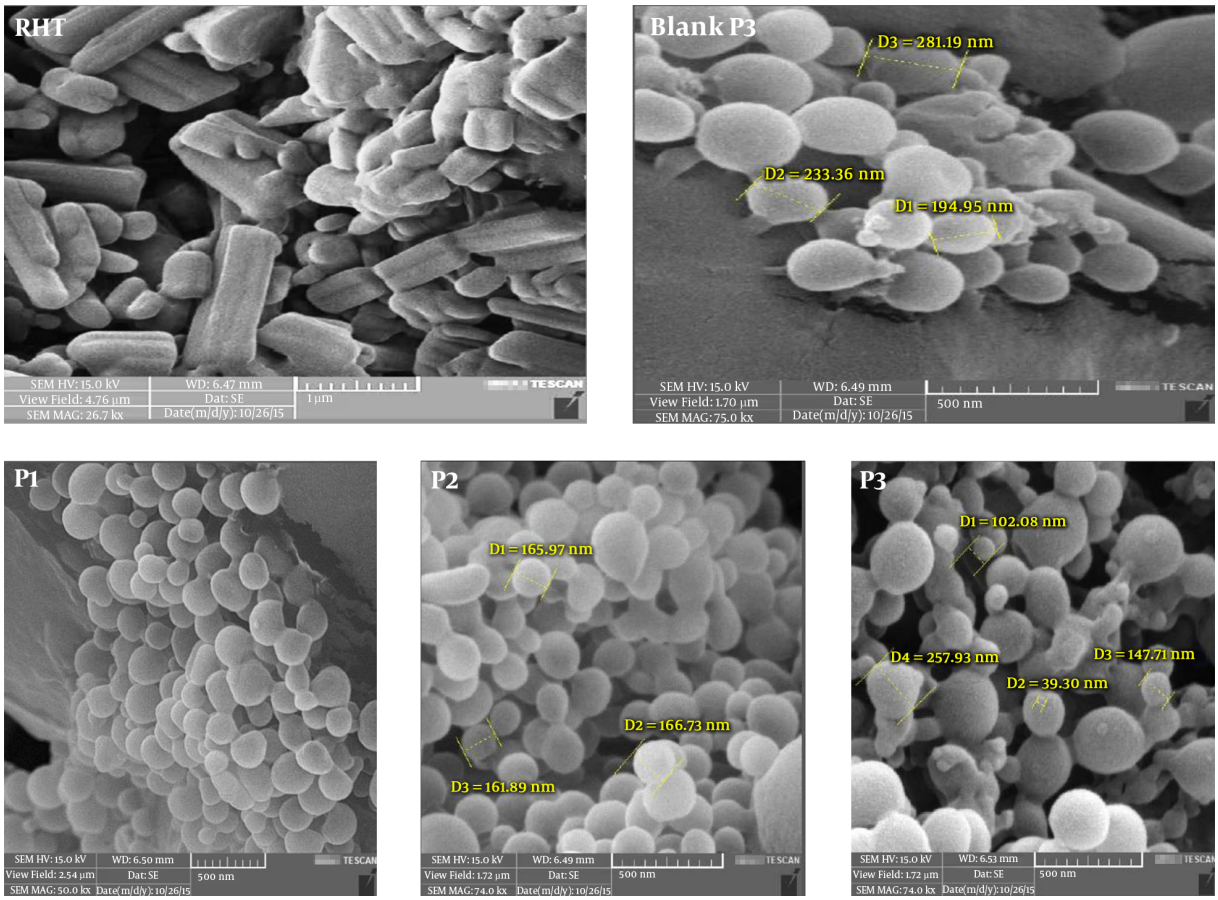

Figure 2. SEM images of RHT, P3 blank, RHT NPs: P1 (PLGA:RHT) 5:1 ratio, P2 (PLGA:RHT) 7:1 ratio, and P3 (PLGA:RHT) 9:1 ratio at 1000 × magnification.

4.3. Evaluation of Polymer-Drug Interaction

4.3.1. Fourier Transform Infrared Spectroscopy

The most obvious characteristic of RHT is ester groups and tertiary amines in the structure of the drug and carboxyl groups and hydroxyl hydrogen tartrate can be noted. Bands at 3319.88 cm^{-1} are attributed to C=O (Figure 3). The characteristic absorption peaks of RHT, obtained at 3319.88 cm^{-1} and 2974.66 cm^{-1}, are related to the stretching vibration bands of C-H. The FTIR spectrum of RHT was the same as that informed by Benkic et al. (11) for polymorph I, with the carbamate band at 1725 cm^{-1}. Stretching bands of C=C appeared at 1403.11 cm^{-1} on the aromatic ring of the drug.

In FTIR spectra of the PLGA polymer, there are also stretching bands in view of C-H stretches at 2885 - 3010 cm^{-1},

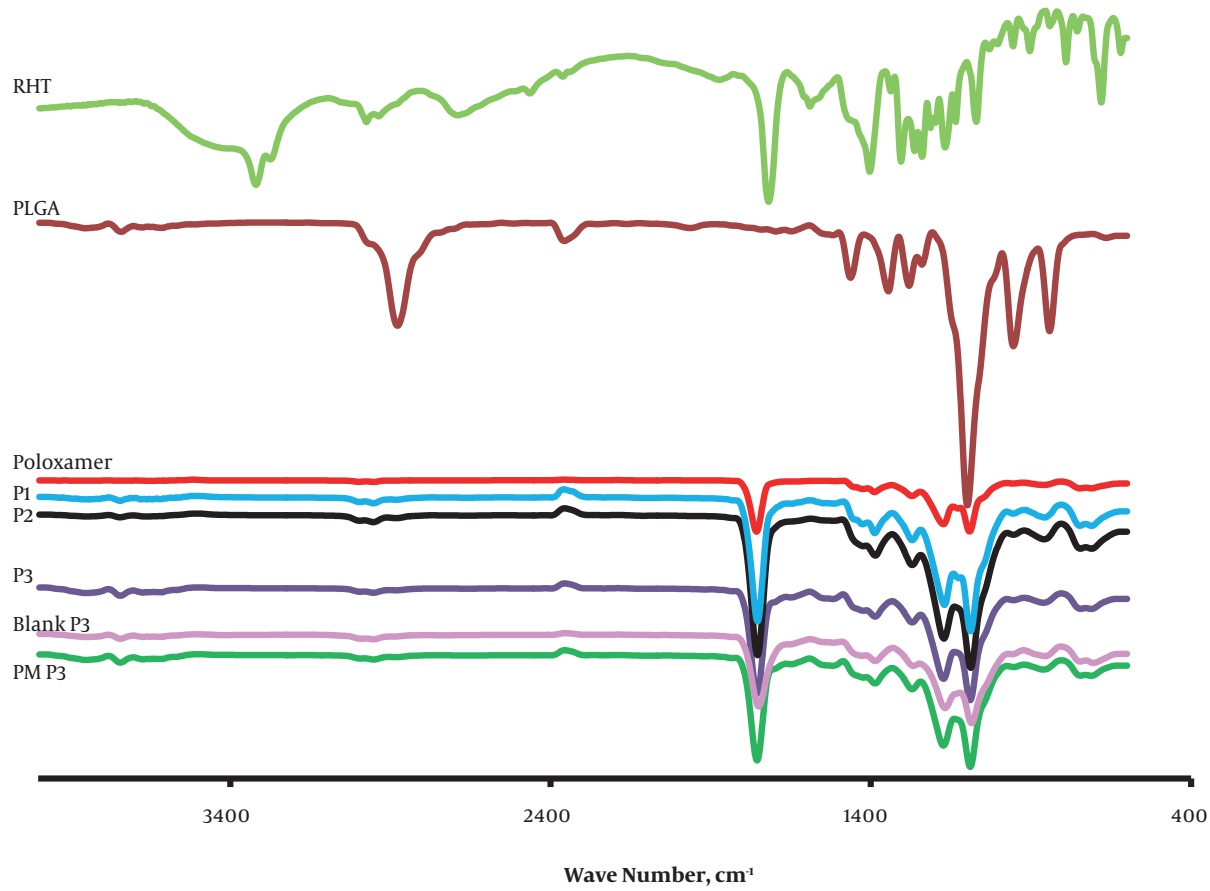

Figure 3. FTIR thermogram of RHT; poloxamer 407; PLGA; P1, P2, P3, blank P3, and physical mixture P3.

C=O stretching at 1759.85 cm^{-1}, C-H bending at 1388.87 cm^{-1} and stretching vibration bands of C-O-C at range 1186 - 1089 cm^{-1}.

The FTIR spectra of poloxamer 407 displayed the major absorption bands at 2885.42 cm^{-1} (C-H stretch aliphatic), 1355.86 cm^{-1} (in-plane O-H bend), and 1112.89 cm^{-1} (C-O stretch) (12). For NPs, stretching vibration C-H was seen at 2953.63 - 2954.36 cm^{-1}, stretch of the carbonyl groups (C=C) at 1752.91 - 1753.58 cm^{-1} (characteristic peak of carbamate), and asymmetric and symmetric C-C (=O)-O vibrations at 1300 to 1150 cm^{-1}. This peak of RHT band of carbamate at range 1752 - 1754 cm^{-1}) was found to merge with the strong CO stretch of the polymer. These data prove that there were chemical interplays in the solid state between the drug and polymer.

Significant alteration was observed in the absorption spectra of physical mixture, as the consist of drug into the PLGA shift the site of functional groups. C-H stretching in RHT appeared at 2974.66 cm^{-1}, which disappeared in the physical mixture and NPs, indicating existence of different association of RHT with the PLGA polymer. This might be because of the delusional effect of the polymer as that of the drug concentration. In the FTIR spectra of the blank NPs of P3, peaks were observed at all the main absorption bands of PLGA (except O-H stretching at 3672.83 cm^{-1}, in-plane O-H bend at 1355.86 cm^{-1}) and poloxamer.

4.3.2. Differential Scanning Calorimetry Analysis

The pure RHT demonstrated a sharp peak at 126.22°C, which can be related to its melting point (Figure 4). Differential Scanning Calorimetry curves were also in agreement with the observed Tg of PLGA (between 40°C and 60°C). Poloxamer 407 showed an endothermic peak (T_m) at 52.76°C. The DSC study declares the status of encapsulated drug either as distributed in a microcrystalline form, without polymorphic change, or with a transitional change in amorphous form (13). The RHT formulations showed an endothermic peak of PLGA at the range of 52.5 to 57.5°C. In the

thermogram of the blank, there was a small endothermic peak at 55.06°C, which correlates with the phase transition of poloxamer and PLGA.

4.3.3. P-XRD Analysis

The X-ray diffraction pattern revealed that the pure drug is crystalline (Form I) in character and has characteristic diffraction peaks at 2Θ values of 5.2, 14.8, 18.8, 20.6, and 21.2° (Figure 5). Poloxamer 407 showed a crystalline nature and manifested several distinct peaks at 13°, 18.5°, 23°, 26°, 35.5°, 39°, and 43°. No peak was observed for the PLGA. Therefore, the results confirmed its amorphous state (14). A change observed in intensity of the peak is shown in Figure 6, which may be ascribed to the distribution of the drug at the molecular level conducting to lower level of finding. When the NPs are prepared, it is obvious that the NPs with higher amount of polymer show the same peaks as the blank NPs. Absence of drug peaks in the physical mixture may be due to the low concentration of RHT in the physical mixture or melting or dissolving of RHT in the polymer during the heating process.

4.4. In Vitro Release Study

The cumulative percentage of drug release from the RHT NPs was occurred in a sustained manner over 24 hours (Figure 6).

5. Discussion

Nano-precipitation is a versatile process based on pouring of an organic solution containing the drug and polymer into a dispersion phase that is miscible with the diffusing solvent yet non-solvent to the polymer (15).

Fessi et al. (7) reported the preparation of NPs by interfacial agitation produced through the diffusion of water-miscible solvent in the water. Having injected the organic phase into the water, a fast interfacial spreading was observed because of the mutual diffusion between the solvents, which supplies energy for oil droplet formation.

Here, the encapsulation efficiency was enhanced from 27.71% to 45.70%, as the amount of the polymer increased from 83.33% to 90%, which can be explained in three methods: Initially, the polymer precipitates quicker on the surface of the dispersed phase at high concentration, and inhibits drug diffusion through the phase boundary. Later, the viscosity of the solution is increased and diffusion of the drug into the polymer droplets is delayed at high concentration. Third, the large size of NPs can result in high concentration of polymer, leading to the loss of drug from the surface during NP washing as compared to the small NPs. Thus, size of NPs also affects the loading efficiency (16).

The small efficiency of drug incorporation can be ascribed to the water soluble properties of RHT.

Thereafter, entrapment of drug decreased from 45.70% to 27.71% (as P3 to P1) with further increases in the theoretical drug loading (from 10% to 16.67%). These results propose that there can be a relatively high amount of RHT that might be entrapped in the PLGA NPs (Figure 3).

Crystal morphology of RHT (Figure 2) showed a plate-like shape for form I. Besides, SEM studies showed that NPs are spherical and discrete in shape. Clearly, high RHT loadings reversely resulted the precipitation of PLGA polymer due to the production of spherical particles.

Zeta potential determinations showed low increases (from -10.5 mV to -2.28 mV) with an increase in polymer concentration (Table 2). These results are the opposite of what was anticipated, which is reduction in surface negativity owing to the interaction of carboxyl groups and the cationic drug on the particle surface. Blank NPs exhibited a negative surface charge of -11.1 mV, which might be due to the appearance of end carboxyl groups of the polymer at the NP surface, as formerly shown for drug-free NPs. An increased negative surface charge was also exhibited by Redhead (17) for Rose Bengal incorporation into PLGA NPs.

Notably, an increase in the theoretical drug loading from 10% to 16.67% w/w results in particle size reduction from 173 nm to 75.14 nm (Table 2). The size of NPs was found to increase with increasing concentration of polymer due to the increase in the viscosity of the organic phase, which renders solvent diffusion more difficult and results in larger NPs size. Average particle size of blank NPs was detected to be approximately the same to that of NPs containing the drug (154 nm).

The results of Table 2 suggest that the size of NPs can be tuned within a range of 75.14 - 173 nm with PDI (0.095 - 0.557). Particles produced with low PLGA concentration (10 mg/mL) were almost monodispersed (P1), showing a PDI of less than 0.1. However, the PDI steadily increased to more than 0.5 in a system with 18 mg/mL of PLGA. A decrease in NPs recovery was observed for NPs produced with different PLGA concentration (from P1 to P3). However, it may result from the increase of particle size as well as from the visually observed aggregation of the already formed particles as evidenced by the PDI value of 0.441 and 0.557 (for P2 and P3, respectively). The current study found that the recovery yield was also dependent on the PLGA concentration in the solvent phase.

The RHT formulations showed complete absence of

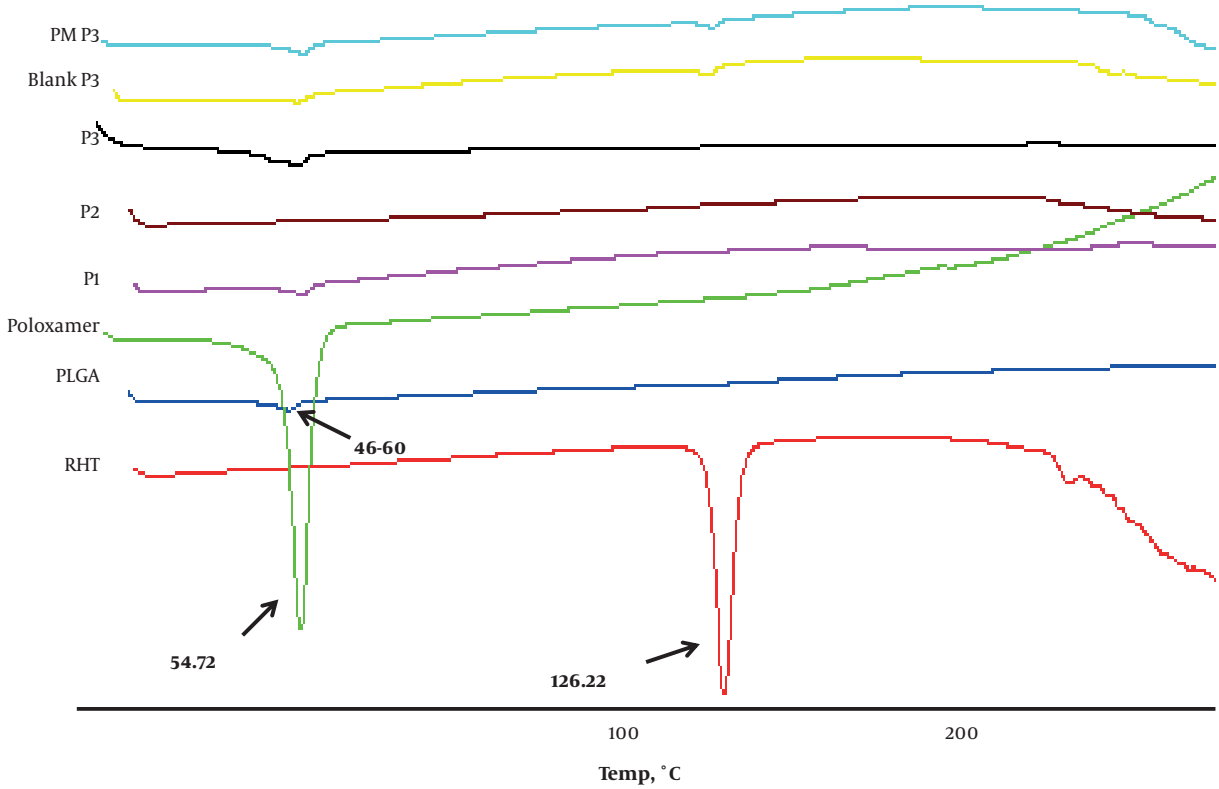

Figure 4. DSC thermogram of RHT; PLGA; poloxamer 407; P1, P2, P3, blank P3, and physical mixture P3.

the drug endotherm and an endothermic peak of PLGA was found at the range of 52.5 to 57.5°C. Besides, the peak at 126.22°C shown by RHT disappeared in the RHT NPs, indicating that RHT was encapsulated by the PLGA polymer. The loss of drug endotherm might be because of the perfect homogeneous matrix organization of the polymer with the drug or to the delusional effect of the polymer (Figure 4).

There may also be the possibility of overlapping of drug peaks by the background diffraction pattern of the amorphous structure (18). Thus, it can be concluded that the drug is present inside the NPs in the semi-crystalline to microcrystalline form. This finding was also in agreement with the rivastigmine tartrate (RT) loaded PLGA polymer nano-suspension, prepared by Joshi et al. (19).

By increasing the PLGA weight fraction from P1 to P3, the potency of typical drug peaks was decreased because of the delusional effect used by the polymer network. This supports the results obtained from FTIR and DSC.

The release behavior of RHT, illustrated in Figure 6, indicates a biphasic pattern (with an initial burst release followed by sustained release). Nano-particles released 9.58 - 21.95% of RHT (for P3 to P1) within 0.5 hours, which had a relationship with the onset of action (Table 3). Afterwards, the NPs exhibited considerable sustained release outcome by lengthening the release of drug at 69.98 - 89% for 24 hours. Using of the polymer PLGA significantly influences drug sustained release (69.98 $\pm$ 4.94%) over an extended time, yet the initial drug release of more than 21.95% within 0.5 hours may be ascribed to the portion of unencapsulated drug inward the polymer (Table 3). At first, the pure drug showed a risen release of RHT in comparison to the NPs, and after 0.5 hours it reached 101.20% ($P < 0.05$). The cumulative release was steady for the pure drug as observed, and did not increment with enhanced time, which improves the value of sustained release characteristic of the NPs. Enhanced drug release (89% $\pm$ 1.51) is associated with increased solubility, which may be due to the fact that

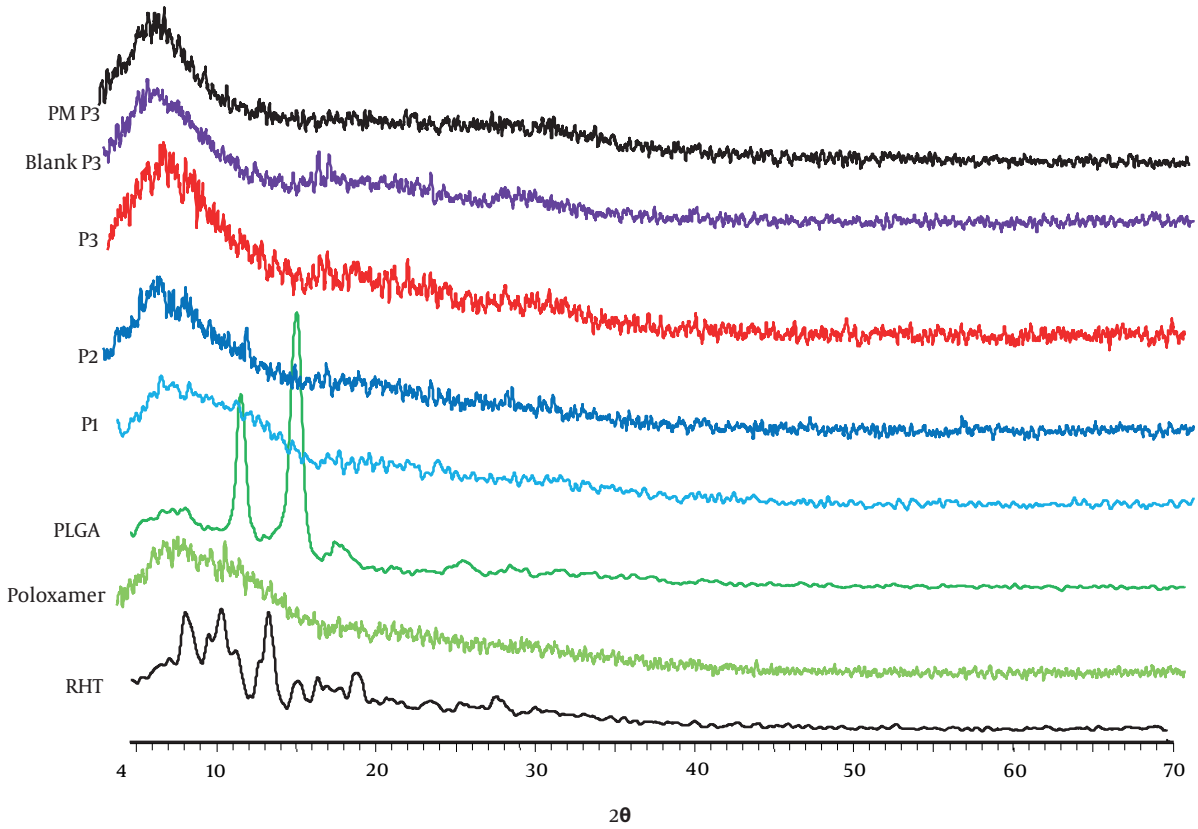

Figure 5. XRD thermogram of RHT; PLGA; poloxamer 407; P1, P2, P3, blank P3, and physical mixture P3.

lower particle size (75.14 nm) of the NPs (P1) effected an increment in the efficient surface area, which in turn increased the solubility (Tables 2 and 3). It is believed that the particle size is inversely proportional to the rate of dissolution and hence a higher rate of dissolution ($P_1 > P_2 > P_3$) was observed with the NPs.

Furthermore, RHT NPs (P1) with lower PLGA showed higher dissolution efficiency and low Mid Dissolution Time (MDT) of 79.44% and 154.79 minutes, respectively (Table 3).

The drug was very gradually released at a later stage, the rate at which was measured by the diffusion ($n < 0.5$) of the drug in the inflexible structure of the matrix. The drug release following the Peppas kinetics and n values exhibited that it was a non-Fickian diffusion mechanism when the drug release occurred. Peppas kinetic model (Table 3) showed the highest correlation; as it is evident from the values of regression coefficients (R^2) for P_1, P_2, and P_3 NPs as 0.915, 0.964, and 0.974, respectively.

Multiple mechanisms, such as swelling, erosion, polymer relaxation, etc. might play a role in the drug release. This could be because rapid dissolution of poloxamer 407 from the surface of NPs created pores or channels and further drug release might have occurred through these pores or channels rather than by erosion. At the final dissolution, the rate of drug release was reduced with time due to the increment in the diffusion path length of the drug.

Acknowledgments

The financial support from the Research Council of Tabriz University of Medical Sciences (under the grant No.110) is greatly acknowledged.

Footnotes

Funding/Support: The financial support from the Research Council of Tabriz University of Medical Sciences (under the grant No.110 is greatly acknowledged.

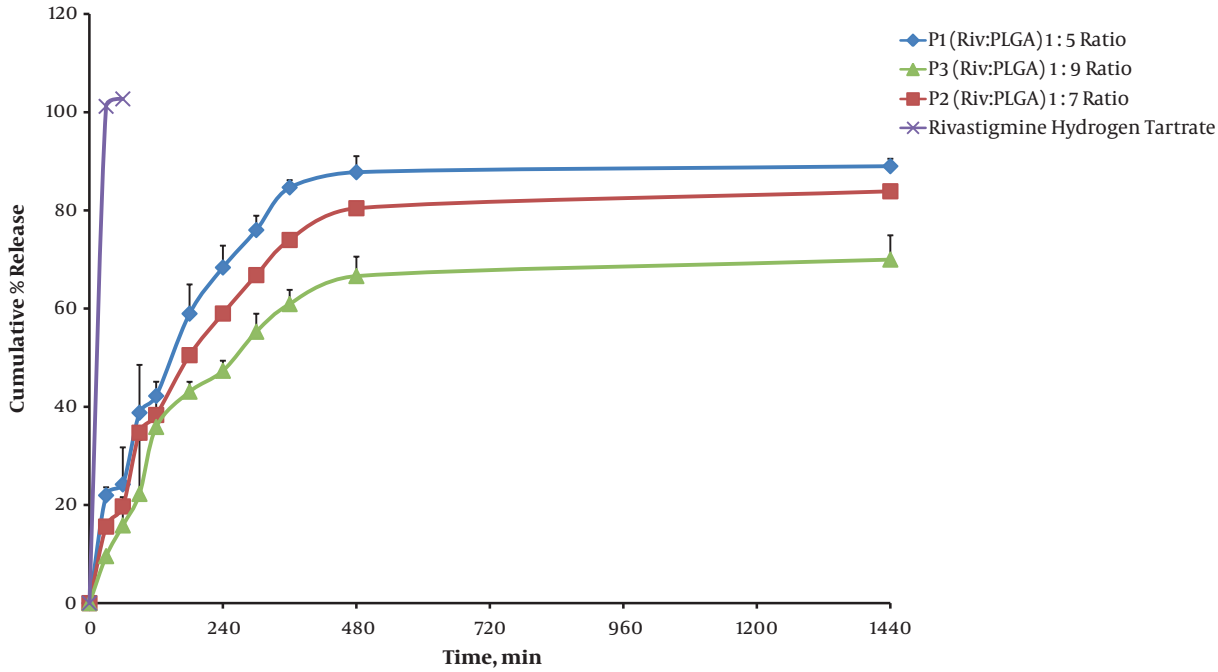

Figure 6. Cumulative percent of RHT release from NPs with different polymer ratios and RHT untreated.

Table 3. Comparison of Various Release Characteristics of RHT from Different NP Formulations and RHT Untreated and Fitting Parameters of the Release Data to Various Kinetic Models

Formulation	$Rel_{0.5}$, %	Rel_{24}, %	DE	$T_{50\%}$, min	f_1	ORDER	RSQ	n
P1	21.95 ± 1.64	89.00 ± 1.51	79.44	154.79	42.29	Peppas	0.915	0.572
P2	15.59 ± 1.34	83.89 ± 8.88	72.76	191.19	49.01	Peppas	0.964	0.680
P3	9.58 ± 0.31	69.98 ± 4.94	60.31	199.15	58.39	Peppa	0.974	0.787
RHT untreated	101.20 ± 7.05	102.71 ± 7.15	101.61	15.44	0	-		

Abbreviations: $Rel_{0.25}$, amount of drug release after 0.5 hours; Rel, amount of drug release after 24 hours; DE, dissolution efficiency; $T_{50\%}$, dissolution time for 50% fractions; f_1, Differential factor ($0 < f_1 < 15$).

Conflict of Interests: The authors declare no conflict of interests.

References

1. Di Stefano A, Iannitelli A, Laserra S, Sozio P. Drug delivery strategies for Alzheimer's disease treatment. *Expert Opin Drug Deliv*. 2011;**8**(5):581–603. doi: 10.1517/17425247.2011.561311. [PubMed: 21391862].
2. Jain KK. Nanobiotechnology-based strategies for crossing the blood-brain barrier. *Nanomedicine (Lond)*. 2012;**7**(8):1225–33. doi: 10.2217/nnm.12.86. [PubMed: 22931448].
3. Salatin S, Maleki Dizaj S, Yari Khosroushahi A. Effect of the surface modification, size, and shape on cellular uptake of nanoparticles. *Cell Biol Int*. 2015;**39**(8):881–90. doi: 10.1002/cbin.10459. [PubMed: 25790433].
4. Dizaj SM, Vazifehasl Z, Salatin S, Adibkia K, Javadzadeh Y. Nanosizing of drugs: Effect on dissolution rate. *Res Pharm Sci*. 2015;**10**(2):95–108. [PubMed: 26487886]. [PubMed Central: PMC4584458].
5. Salatin S, Jelvehgari M, Maleki-Dizaj S, Adibkia K. A sight on protein-based nanoparticles as drug/gene delivery systems. *Ther Deliv*. 2015;**6**(8):1017–29. doi: 10.4155/tde.15.28. [PubMed: 26305428].
6. Tosi G, Bortot B, Ruozi B, Dolcetta D, Vandelli MA, Forni F, et al. Potential use of polymeric nanoparticles for drug delivery across the blood-brain barrier. *Curr Med Chem*. 2013;**20**(17):2212–25. doi: 10.2174/0929867311320170006. [PubMed: 23458620].
7. Fessi HPFD, Puisieux F, Devissaguet JP, Ammoury N, Benita S. Nanocapsule formation by interfacial polymer deposition following solvent displacement. *Int J Pharm*. 1989;**55**(1):R1–4. doi: 10.1016/0378-5173(89)90281-0.
8. Quintanar-Guerrero D, Allemann E, Fessi H, Doelker E. Preparation techniques and mechanisms of formation of biodegradable nanoparticles from preformed polymers. *Drug Dev Ind Pharm*. 1998;**24**(12):1113–28. doi: 10.3109/03639049809108571. [PubMed: 9876569].
9. Sharma D, Maheshwari D, Philip G, Rana R, Bhatia S, Singh M, et al. Formulation and optimization of polymeric nanoparticles for intranasal

delivery of lorazepam using Box-Behnken design: In vitro and in vivo evaluation. *Biomed Res Int*. 2014;**2014**:156010. doi: 10.1155/2014/156010. [PubMed: 25126544]. [PubMed Central: PMC4122152].
10. Loveymi BD, Jelvehgari M, Zakeri-Milani P, Valizadeh H. Design of vancomycin RS-100 nanoparticles in order to increase the intestinal permeability. *Adv Pharm Bull*. 2012;**2**(1):43–56. doi: 10.5681/apb.2012.007. [PubMed: 24312770]. [PubMed Central: PMC3846008].
11. Benkic P, Smrkolj M, Pecavar A, Stropnik T, Vrbinc M, Vrecer F, et al. Amorphous and crystalline forms of rivastigmine hydrogen tartrate. *Eur Pat Applic*. 2008:1–30.
12. Liu J, Qiu Z, Wang S, Zhou L, Zhang S. A modified double-emulsion method for the preparation of daunorubicin-loaded polymeric nanoparticle with enhanced in vitro anti-tumor activity. *Biomed Mater*. 2010;**5**(6):65002. doi: 10.1088/1748-6041/5/6/065002. [PubMed: 20924138].
13. Derman S. Caffeic acid phenethyl ester loaded PLGA nanoparticles: effect of various process parameters on reaction yield, encapsulation efficiency, and particle size. *J Nanomaterials*. 2015;**16**(1):318. doi: 10.1080/10915810802244595.
14. Domanska U, Halayqa M. Promazine Hydrochloride/PLGA biodegradable nanoparticles formulation and release. *J Phys Chem Biophys*. 2014;**4**(2):1000143. doi: 10.4172/2161-0398.1000143.
15. Tefas LR, Tomuta I, Achim M, Vlase L. Development and optimization of quercetin-loaded PLGA nanoparticles by experimental design. *Clujul Med*. 2015;**88**(2):214–23. doi: 10.15386/cjmed-418. [PubMed: 26528074]. [PubMed Central: PMC4576773].
16. Salatin S, Barar J, Barzegar-Jalali M, Adibkia K, Kiafar F, Jelvehgari M. Development of a nanoprecipitation method for the entrapment of a very water soluble drug into Eudragit RL nanoparticles. *Res Pharm Sci*. 2017;**12**(1):1. doi: 10.4103/1735-5362.199041. [PubMed: 28255308]. [PubMed Central: PMC5333474].
17. Amaro MI, Simon A, Cabral LM, de Sousa VP, Healy AM. Rivastigmine hydrogen tartrate polymorphs: Solid-state characterisation of transition and polymorphic conversion via milling. *Solid State Sci*. 2015;**49**:29–36. doi: 10.1016/j.solidstatesciences.2015.09.004.
18. Graeser KA, Strachan CJ, Patterson JE, Gordon KC, Rades T. Physicochemical properties and stability of two differently prepared amorphous forms of simvastatin. *Crystal Growth Design*. 2008;**8**(1):128–35. doi: 10.1021/cg700913m.
19. Joshi SA, Chavhan SS, Sawant KK. Rivastigmine-loaded PLGA and PBCA nanoparticles: preparation, optimization, characterization, in vitro and pharmacodynamic studies. *Eur J Pharm Biopharm*. 2010;**76**(2):189–99. doi: 10.1016/j.ejpb.2010.07.007. [PubMed: 20637869].